Cloud-Resolving Modeling of Deep Convection during KWAJEX. Part I: Comparison to TRMM Satellite and Ground-Based Radar Observations

Yaping Li, Edward J. Zipser, Steven K. Krueger, and Mike A. Zulauf

Department of Meteorology, University of Utah, Salt Lake City, UT

Manuscript prepared for

Monthly Weather Review

Submission Date: April 26, 2007
Revision Date: September 24, 2007
Revision Date: November 14, 2007

Corresponding author address:
Yaping Li
IMSG at NOAA/NESDIS/STAR
5200 Auth Rd.
Camp Spring, MD 20746
Email: Yaping.Li@noaa.gov

Abstract

A global TRMM database of tropical cloud system precipitation features (PFs), which provides useful observational constraints on cloud system properties, is used to evaluate the bulk microphysics schemes in a cloud-resolving model (CRM). The simulation of the Mesoscale Convective System (MCS) of 11-12 August 1999 during the Kwajalein Experiment (KWAJEX) is executed using the 3-D University of Utah CRM, which employs a one-moment bulk, three-ice category microphysical parameterization. The simulated precipitation features are compared with climatological "norms" for Kwajalein locations from the TRMM PF database to evaluate the precipitation microphysics of the cloud model simulation. The model simulated reflectivities are also compared with vertical profiles of radar reflectivity obtained from a ground-based precipitation radar.

Comparison of simulation results with the TRMM observation statistics indicates that the model tends to underestimate microwave brightness temperatures at ice scattering frequencies and overestimate radar reflectivities, especially for those associated with larger ice particles. The differences between the statistics of KWAJEX simulation and available ground-based precipitation radar observations are relatively small at the levels below 5 km. Above 6 km, the differences increase with height and reach a maximum near 9 km. The simulated radar reflectivities are statistically 5-13 dBZ higher than those from radar observations at levels between 7 and 10.5 km, where graupel is the dominant simulated ice species. The largest graupel mixing ratios, as high as 8 g kg^{-1}, are the most likely reason for the unrealistically high simulated radar reflectivity. Comparison of model simulated graupel mixing ratio with available microphysics data from the Citation aircraft indicates that the model overestimates graupel content at the level the Citation flew (about 6.4 km).

1. Introduction

Cloud microphysics is one of the most important factors in the lifecycle of convective cloud systems because of the interaction of cloud microphysics with cloud dynamics and radiation. The release of latent heat during condensation, sublimation and freezing produces buoyancy that drives updrafts while hydrometeor mass loading reduces the buoyancy, and downdrafts are generated by precipitation drag, and by latent cooling due to evaporating liquid water particles and/or melting ice particles. The important role of cloud microphysical processes in convective system simulations has been clearly shown in a number of previous modeling studies (e.g., Lord et al. 1984; McCumber et al. 1991; Fu et al. 1995; Krueger et al. 1995; Prasad et al. 1995; Yeh et al. 1995; Simpson et al. 1996; Brown and Swann 1997; Grabowski et al. 1999; Wang 2002; Tao et al. 2003; McFarquhar et al. 2006; Lang et al. 2007).

In addition, microphysics parameterization is especially important when cloud resolving models (CRMs) are used for remote sensing applications. The accuracy of cloud and precipitation retrievals for a large number of instruments on satellites and aircraft depends on the ability of cloud resolving models to provide the three-dimensional (3-D) distribution of microphysical properties of the precipitating cloud that is consistent with the observations.

With increased computational ability, CRMs are able to incorporate more sophisticated microphysics parameterizations (e.g., multiple-moment schemes and bin microphysics) for simulating cloud formation and evolution. Bin microphysical models explicitly calculate particle number concentration in different size categories (e.g., Hall 1980; Khain et al. 1996, 1999, 2000; Ovtchinnikov and Kogan 2000; Khain et al. 2001, 2004; Lynn et al. 2005). This leads to large numbers of predicted variables and high computational expense, especially for 3D models. In contrast, bulk-microphysics schemes (e.g., Lin et al. 1983; Rutledge and Hobbs 1984; McCumber et al. 1991; Schultz 1995; Reisner et al. 1998; Tao et al. 2003), employ a simple integrable statistical distribution of hydrometeors, such as the Marshall and Palmer (1948) raindrop size

distribution, which makes the bulk parameterization computationally more efficient, with 1-2 orders of magnitude less computational expense. Multiple-moment bulk schemes (e.g., Ferrier 1994; Meyers et al. 1997; Reisner et al. 1998; Morrison et al. 2005; Milbrandt and Yau 2005) improve calculations of the microphysical processes and providing more microphysical details than single-moment bulk schemes (Meyers et al. 1997). However, they are computationally more expensive and more sensitive to small perturbations in the initial conditions (Ferrier 2003). In order to prevent decoupling of mixing ratio from number concentration, an accurate, positive-definite advection scheme is required (Tao et al. 2003 and Johnson et al. 2002). Therefore, single-moment parameterizations are still widely used in cloud resolving models, numerical weather prediction models and general circulation models because of their simplicity and computational efficiency.

The evaluation of bulk microphysics schemes in numerical models is an important but tough task, because of the complexity of clouds and the large range of relevant space and time scales. Microphysical parameterizations in CRMs are often evaluated using case studies by comparing the simulation results with in situ microphysical measurements that are collected during field experiments (e.g., Brown and Swann 1997). These studies are valuable. However, given the limited temporal and spatial sampling of the in situ microphysical measurements, even during extensive campaigns, assessments of the highly variable cloud fields are bare. In contrast, observations from satellites offer good coverage in time and space. Therefore, model vs. satellite approaches have been used, in which modeled cloud fields are compared with cloud quantities retrieved from satellite-borne sensors (e.g., Yeh et al. 1995; Prasad et al. 1995; Simpson et al. 1996; Chaboureau et al. 2000 and 2002; Krueger and Luo 2007), or simulated radiances using output from the model are compared to satellite observed radiances (e.g., Wiedner et al. 2004; Lang et al. 2007). However, it is often difficult to separate errors in the cloud model microphysics from those related to the forcing used to drive the CRM or assumptions employed in satellite

retrievals. Therefore, direct comparisons between simulated radiances and satellite observations have some advantages for a systematic evaluation of atmospheric models. The sensitivity of passive microwave radiances to precipitating ice particles make it possible to quantitatively assess the ice content generated by the cloud model. However desirable, it is not necessary to obtain corresponding satellite observations for every special case to evaluate simulation results.

The global Tropical Rainfall Measuring Mission (TRMM) database of tropical cloud system precipitation features (PFs; Nesbitt et al. 2000) at the University of Utah provides useful observational constraints on cloud system properties. Precipitation features are defined by utilizing a combination of the Precipitation Radar (PR) near-surface reflectivity and the TRMM Microwave Imager (TMI) 85-GHz polarization corrected temperature (PCT; Spencer et al. 1989). The features are then classified by their size and intensity of the 85-GHz ice scattering signatures into three categories: *precipitation features without ice scattering* (no pixels containing PCT $\leq$ 250 K at 85 GHz); *precipitation features with ice scattering* (at least one pixel with 85-GHz PCT $\leq$ 250 K), and *precipitation features with a mesoscale convective system* (at least 2000 km^2 of contiguous area with 85-GHz PCT $\leq$ 250 K and 185 km^2 with 85-GHz PCT $\leq$ 225 K). This TRMM PF database has been used in several studies (e.g., Nesbitt et al. 2000; Toracinta et al. 2002; Li 2003) to present analyses of the global and/or regional distributions of discrete precipitation features. This study uses this unique TRMM database to help evaluate the bulk microphysics schemes in a cloud-resolving model.

We simulated a mesoscale convective system (MCS) observed during the Kwajalein Experiment (KWAJEX, Yuter et al. 2005) using the 3-D University of Utah cloud resolving model. We calculated brightness temperatures using modeled hydrometeor fields as input to a microwave radiative transfer model (Kummerow and Weinman 1988). Simulated radar reflectivities are calculated using the relations of Smith et al. (1975) and Smith (1984) from modeled fields. Based on the simulated 85-GHz brightness temperature and radar reflectivity, the

simulated precipitation features are defined in a way that is consistent with those in the TRMM database, and then compared with climatological "norms" for Kwajalein locations from the TRMM PF database to evaluate the precipitation microphysics of the cloud model simulation. The simulated reflectivities are also compared with vertical profiles of radar reflectivity obtained from a ground-based precipitation radar.

The main purpose of this paper is to show an example of how the TRMM PF and ground-based radar observations can be used to suggest reasonable observational constraints on cloud system properties and to help evaluate the bulk microphysics schemes in the numerical model. In this paper, we focus on a single large MCS and not on the full spectrum of convective feature sizes. The paper is organized as follows. The next section describes the Kwajalein Experiment (KWAJEX), and the TRMM-observed statistical characteristics of MCSs in the region of Kwajalein which provide a climatological context for the MCS observed during KWAJEX. The convective system selected for investigation is also described in this section. Section 3 presents a summary of the cloud-resolving model used in this study and the experimental setup. Section 4 presents the simulation results and statistical comparisons of the simulated and observed convective radar reflectivity and microwave brightness temperature. Conclusions are given in section 5.

2. Case description

a. KWAJEX

The Kwajalein Experiment (KWAJEX) was centered on Kwajalein Atoll in the Republic of the Marshall Islands and took place during the period 23 July-15 September 1999. It was one of several field campaigns that comprised the NASA TRMM ground validation program that was designed to address particular issues related to the remote measurements made by instruments on the TRMM satellite. The KWAJEX measurements were taken from three aircraft, five upper-air

sounding sites, one ship and a collection of remote and in situ surface-based sensors, including scanning Doppler radars, profilers, disdrometers, and rain gauges (Yuter et al. 2005). The Kwajalein S-band radar was particularly important, as it was used to obtain information about the 3-D precipitation structure, to supply high quality estimates of area-averaged precipitation rates, and to vector aircraft to specific locations within storms during research aircraft operations. During the whole experiment time period, isolated convective systems of small horizontal dimension were prevalent (Cetrone and Houze 2006). Three of the days included broad MCSs that moved through the KWAJEX domain (25-26 July, 11-12 August, and 2-3 September). A detailed description of these three precipitation events and their relation to the large-scale meteorological conditions are found in Sobel et al. (2004).

b. Climatological characteristics of Kwajalein MCS

In order to provide a climatological context for the MCS observed in KWAJEX, a database of TRMM observations of precipitation features (PFs; Nesbitt et al. 2000) is built from 5.5˚ – 12˚N and 164˚ – 172˚E for the rainy seasons in 1998, 1999, 2000, 2002 and 2003. The Kwajalein rainy season begins in May or June. For this study, the months of July - September are selected so that the periods are comparable to the KWAJEX IOP. The sample size includes 18924 precipitation features, of which 17274 are features without ice scattering, 1542 features with ice scattering and 108 features with MCS. Here the subset that includes only MCSs, which are not representative for the vast majority of convection that forms near Kwajalein, is examined. Statistics related to the intensities of the TRMM-observed Kwajalein MCSs are analyzed, including the cumulative distribution functions (CDFs) of minimum 85- and 37-GHz PCT, maximum height of the 20- and 40- dBZ echo and maximum 6- and 9-km reflectivity (Figure 1).

Figure 1 shows that the TRMM observed Kwajalein MCSs have a median minimum 85-GHz PCT of 160 K. The corresponding value for 37-GHz is 255 K. The maximum heights of the

20-dBZ are 9.5 – 16.5 km. About 20% have values greater than 15 km. The maximum heights of the 40-dBZ echoes are less than 8 km. The median maximum reflectivities at 6 km reach 37.5 dBZ. About 80% have a maximum reflectivity at 6-km between 34 and 45 dBZ. The MCSs have a median maximum 9-km reflectivity of 29 dBZ, while more than 25% MCSs have values greater than 30 dBZ. These statistics are typical of oceanic regions around the tropics (e.g., Nesbitt et al. 2000; Toracinta et al. 2002), and signify that the convective regions of these MCSs are of only moderate intensity.

Compared to the analogous statistics for four other well-studied tropical regions (Florida area, GATE area, TOGA COARE area, and TRMM-LBA area) in Li (2003), these values are closest to those for the TOGA COARE area. But these large MCSs are quite rare near Kwajalein, and more common in the TOGA COARE region and elsewhere in the tropics.

c. The Kwajalein MCS of 11-12 August 1999

The 11-12 August 1999 convective system, which was the best-sampled large mesoscale precipitation system during KWAJEX, is simulated in this study. This MCS was associated with the interaction between a westward-propagating mixed Rossby gravity wave and an eastward-propagating Kelvin wave that crossed paths near Kwajalein (Sobel et al. 2004). At around 1800 UTC 11 August 1999, strong convection developed to the east of Kwajalein and moved towards the southwest into the observation range of the Kwajalein radar. Over the following several hours, the system evolved from a highly convective state at around 1930 UTC to an almost entirely stratiform state at around 0230 UTC. After that, the system gradually dissipated until there was almost no radar echo remaining by 0600 UTC. The synoptic situation, satellite and radar observations of this case have been described in detail by Spooner (2001).

The frequency distribution of reflectivity within a precipitating cloud system varies with height. Analysis of this height variation [as represented in a contoured cumulative frequency by

altitude diagrams (CCFADs)] provides insight into the structure of cloud system. CCFADs are constructed in a similar manner to the contoured frequency by altitude diagrams of Yuter and Houze (1995), except that the cumulative frequency at each bin and height is calculated. CCFAD of reflectivity observed by the Kwajalein ground-based S-band radar for the 11-12 August 1999 convective system is shown in Figure 2. This CCFAD is accumulated from 2024 UTC 11 August to 0200 UTC 12 August 1999 for the 20- 60-km radius interval to assure good vertical resolution, with a constant bin size of 1 dBZ. Statistics are derived from 56 radar volume scans. Radar data analyzed in this study come from the web site of KWAJEX (http://daac.gsfc.nasa.gov/fieldexp/TRMM_FE/kwajex/). The S-band radar scan strategies and calibration for KWAJEX are described in Yuter et al. (2005). These radar data have been interpolated onto a Cartesian grid covering 312 km × 312 km in the horizontal with a 2 km spacing from 1.5 to18 km MSL in the vertical with 1.5 km spacing. In this study, the Kwajalein radar data have been normalized to be comparable to the TRMM Precipitation Radar footprint of 4 km. Only the columns with lowest level reflectivity greater than or equal to 20 dBZ are selected for analysis. (20 dBZ is chosen in order to make it consistent with the way we analyze TRMM precipitation features, i.e., contiguous near-surface echo > 20 dBZ.) This eliminates about a fourth of the samples that were originally present without this restriction. The total number of columns that fulfill the selection criteria is 132123, within the 20-60 km radius interval from the radar.

The overall pattern in the CCFAD (Figure 2) is a rapid decrease of reflectivity with increasing height above the 0°C level (at about 4.5 km). The mode within the rain layer (below the 0°C level) shows increasing reflectivity with decreasing height, especially the profiles of 90%, 99%, 99.9% and 99.99% quantiles, which is consistent with precipitation growth. At the 6 km level, the median radar reflectivity is 22 dBZ and the top 1% ≤ 34 dBZ. From Figure 1, 80% of the TRMM observed MCSs in the region of Kwajalein have a maximum 6-km reflectivity greater than 34 dBZ. For this KWAJEX MCS, the top 1% reflectivity at 6 km is less than 34 dBZ, which

is less than the median value of maximum 6-km reflectivity for the TRMM observed Kwajalein MCSs (37.5 dBZ in Figure 1). From Figure 2, the median radar reflectivity at 9 km for this KWAJEX MCS is 10 dBZ, and the top 1% reflectivity is less than 22 dBZ for this MCS. Figure 1 shows that the median reflectivity at 9 km is about 29 dBZ for the TRMM observed Kwajalein MCSs, and more than 25% have maximum 9-km reflectivity greater than 30 dBZ. From Figure 2, for the height of the 20 dBZ echo, the top 10% value for the KWAJEX 11-12 August 1999 MCS is less than 8 km, with the top 1% value less than 10 km. From Figure 1c, 95% of the TRMM observed MCSs in the region of Kwajalein have the maximum height of the 20 dBZ echo greater than 10 km. Figure 2 shows that the top 1% value of the height of the 40 dBZ echo for this KWAJEX MCS is about 4 km, compared to 95% of the TRMM observed Kwajalein MCSs with the maximum 40-dBZ echo height higher than 4 km. All these comparisons indicate that *this KWAJEX MCS is a weak-to-average system in terms of "proxies" for convective intensity against the 5-year TRMM sampled 108 MCSs in the region of Kwajalein*, although this particular KWAJEX MCS is large in size and rains heavily.

3. Model simulation

a. Model description

The model used in this study is the three-dimensional University of Utah (UU) CRM, which is based upon a nonhydrostatic set of primitive equations and is described in detail in Zulauf (2001) and Garrett et al. (2006). This model is specifically designed to examine small-scale atmospheric flows. Subgrid-scale turbulence is modeled according to Deardorff (1980). A prognostic equation is employed for the subgrid-scale turbulence kinetic energy (TKE) and the subgrid fluxes of momentum and scalar quantities are diagnosed using eddy viscosities derived from the subgrid-scale TKE. Finite differences are used to discretize the governing equations. The time differencing utilizes a time split second-order Runge-Kutta scheme (Wicker and Skamarock,

1998). The momentum advection terms are differenced with a third-order upwind-biased scheme. The modified UTOPIA (Uniform Third-Order Polynomial Interpolation Algorithm) scheme of Stevens and Bretherton (1996) is used for scalar advection, and monotonicity is maintained using the Zalesak's flux-corrected transport (1979). All other terms utilize second-order centered differences.

The CRM utilizes a single-moment, 3-ice bulk microphysical parameterization scheme in which the hydrometeors are categorized into five types: cloud water, cloud ice, rain, snow, and graupel. The parameterized cloud microphysics largely follows Lin et al. (1983) and Lord et al. (1984), but Krueger et al. (1995) improved the ice phase parameterizations by modifying the growth of cloud ice by the Bergeron process, the conversion of cloud ice to snow, and the characteristics of graupel, so that the microphysical processes that occur in tropical cloud clusters can be more realistically simulated (Krueger et al. 1995).

In this single-moment bulk scheme, it is assumed that the terminal velocities of cloud water and cloud ice are insignificant and can be neglected compared with the velocities of air, rain and precipitating ice. Rain, snow, and graupel have mass-weighted mean terminal velocities that depend on the mixing ratio and size distribution assumed. Exponential size distributions are assumed for each precipitation particle:

$$n_\chi(D) = n_{0\chi} \exp(-\lambda_\chi D_x), \tag{1}$$

where $n_{0\chi}$ is the intercept parameter of precipitation particle size distribution, the subscript x denotes rain (R), snow (S) or graupel (G). D_χ is the diameter of a precipitation particle. The slope parameters of precipitation size distributions (λ_χ) are determined by multiplying (1) by particle mass and integrating over all particle diameters and then equating the resulting quantities to the appropriate water contents. The Lin et al. (1983) scheme was originally designed to simulate midlatitude hailstorms and specify $\rho_G = 9.2 \times 10^2$ kg m^{-3} and $n_{0G} = 4 \times 10^4$ m^{-4}. For

tropical convection, Mccumber et al. (1991) concluded that it is better to choose the bulk ice hydrometeor mix to be cloud ice-snow-graupel rather than cloud ice-snow-hail. Therefore, the intercept parameter n_0 and density ρ for graupel given by Rutledge and Hobbs (1984): n_{0G} = 4×10^6 m^{-4} and $\rho_G = 0.4 \times 10^3$ kg m^{-3} are employed in this study. The densities for rain and snow particles are $\rho_R = 1.0 \times 10^3$ kg m^{-3} and $\rho_S = 0.1 \times 10^3$ kg m^{-3}, and the intercept parameters are $n_{0R} = 8 \times 10^6$ m^{-4} and $n_{0S} = 3 \times 10^6$ m^{-4}.

b. Design of model simulation

Since the 3-D cloud-resolving model is computationally expensive, to choose a reasonable horizontal resolution and horizontal domain size for the statistical studies is firstly considered in this study. A series of sensitivity tests have been done, with varying horizontal grid resolution Δx = 250 km, 500 m, and 1000 m and the horizontal domain sizes varying from 64 km x 64 km to 128 km x 128 km. The results revealed that the differences of the convection intensity statistics between the 250 m and 500 m runs are much less than those between the 500 m and 1000 m runs. The results did not reveal that the convection intensity statistics were sensitive to the domain size. [More details about these sensitivity tests can be found in Li (2006)]. Therefore, a horizontal domain of 128 x 128 grid points with a 500-m grid spacing is chosen in this study. A quadratic stretching scheme is employed in the vertical grid, with the spacing increasing from 75 m at the surface to 600 m at the top of the domain (at 27 km). Above the sounding top (at 100 mb, about 16.5 km), the standard Tropical atmosphere is used for the initial conditions, and for the reference profile in the sponge layer (also located above 100 mb). The sponge layer is used to prevent the reflection of upward-propagating gravity waves at the top of the domain.

The simulation is run for 72 h starting at 0000 UTC August 10, 1999 (the first 36-hour is considered as the model spin-up). It is initialized using the observed sounding at 0000 UTC 10

August and driven by the time-varying large-scale forcing (Soong and Ogura 1980; Soong and Tao 1980) taken from the objectively analyzed dataset (Zhang 2003) based on the observations made over the Kwjalein area during the KWAJEX IOP from July 24 to September 14, 1999 and generated using the multivariate constrained optimization method of Zhang et al. 2001. Blossey et al. (2006) used this analysis to perform simulation for the entire 52-day period of KWAJEX. This multivariate constrained optimization method has been used to generate the large-scale forcing database which has been employed in several numerical simulation studies (e.g., Xu et al., 2002; Khairoutdinov and Randall 2003). The large-scale advective tendency profiles for temperature and vapor mixing ratio are imposed on the model grid points uniformly in the horizontal domain and linearly interpolated in time from the 6-h data. The large-scale horizontal advection terms are added directly to the model equations as forcing terms, while the large-scale vertical advection is calculated from the analyzed omega and the predicted vertical gradients. The domain-averaged horizontal wind profile is nudged to the observed horizontal wind profile on a 2-h timescale. The radiative heating rate profile is explicitly calculated using Fu's radiation code (Fu and Liou, 1993; Fu et al. 1995). The surface latent and sensible heat fluxes have been prescribed in the simulations. Periodic lateral boundary conditions are used in both the east-west and north-south directions.

c. Computation of simulated brightness temperature and reflectivity

A radiative transfer model (RTM; Kummerow and Weinman 1988) is used to calculate the microwave upwelling brightness temperature based on the outputs of the cloud resolving model. In the RTM, the general microwave radiative transfer equation is solved based on the one-dimensional Eddington approximation for a multilayered plane parallel medium. The absorption coefficient of the cloud water and cloud ice is computed by using the Rayleigh approximation. Mie theory is employed to compute the absorption and scattering by precipitation-size hydrometeors. Liquid and ice particles are assumed to be spherical. The distributions of cloud

water and cloud ice are assumed to be monodisperse. The densities and exponential intercept parameters are separately set for each precipitation hydrometeor category to match the values used in the CRM. A TRMM-like scanning incidence angle (i.e. 52°) is used in the radiative transfer calculations. The outputs of the RTM include the horizontal and vertical polarization brightness temperatures at 10.7, 19.35, 21.3, 37 and 85.5 GHz.

Reflectivity estimates are generated from the simulation using the mixing ratios of cloud water, cloud ice, rain, snow and graupel. For cloud water and cloud ice, the reflectivity depends on the effective radius of the cloud particles and the mixing ratio, following the relation of Beesley et al. 2000. It is assumed that cloud water droplets have a constant effective radius of 10 μm, and cloud ice particles are assigned a constant generalized effective size of 25 μm (Luo et al. 2003). The simulated reflectivities of snow and graupel are calculated using the methods of Smith et al. (1975) and Smith (1984), in which radar reflectivity depends on the mixing ratio and density of species, as well as the intercept parameter of the hydrometeor distribution.

Simulated microwave brightness temperatures are obtained for each grid box based on the outputs of the cloud resolving model. The cloud resolving model has a horizontal grid area of 500 m × 500 m, which is much smaller than the footprint sizes of TMI 37- and 85-GHz channels, about 9.7 km x 16 km and 4.2 km x 6.9 km, respectively. In order to relate high-resolution model results to actual TRMM observations, the simulated fields are convolved with a Gaussian function that is close to the TMI antenna patterns for each frequency. The horizontal resolution of the TRMM Precipitation Radar is 4.2 km, so the simulated radar reflectivities are degraded from the model's high resolution to TRMM PR's resolution. In order to compare simulated reflectivity to that from ground-based radar observations, the simulated reflectivities are degraded to the corresponding resolution of ground-based radar data (2 km).

4. Comparisons of simulation results to observations

The animation of x-y plots of simulated radar reflectivity for a 12-hour period between 1800 UTC August 11 and 0600 UTC August 12 (not shown) indicates that the simulated convective system moves from east to west, with individual convective cells moving from northwest to southeast. The simulated cell motion and system motion are in good agreement with observations, as shown by the time-lapse radar movie loops from the Kwajalein precipitation radar. The simulated system evolves from a highly convective state in the first 6-7 hours to nearly 100% stratiform from 6-12 hours, similar to the actual MCS. This 12-hour simulation period is analyzed in the following sections. Convective updraft and downdraft cores play very important roles in the transport of mass, momentum, heat and energy. Therefore, whether the model predicts convective vertical velocity realistically is checked first.

a. Simulated updraft and downdraft cores

Using the model output at 15-minute intervals, convective core statistics are generated by flying imaginary aircraft through the modeled system. Simulated convective cores are identified and analyzed using the methodology and definition of a core similar to that used by previous observation studies (e.g., LeMone and Zipser 1980; Zipser and LeMone 1980; Jorgensen et al. 1985; Jorgensen and LeMone 1989; and Lucas et al. 1994). An updraft or downdraft core is defined where the magnitude of the vertical velocity (w) continuously exceeds (or is equal to) 1 m s^{-1} for at least 1 km or two grid points. We arbitrarily take X=6, 18, 30, 42 and 54 km, and Y=6, 18, 30, 42 and 54 km flight tracks across the grid at a given time (10 tracks each time), and repeat for every 1 km in the vertical from 0.5 km to 14.5 km. Using the criteria established above, the number of identified cores varies with height, varying from 109 to 734 for updraft cores, and 25 to 508 for downdraft cores (Figure 3). For the simulated updraft and downdraft cores, several characteristics are computed, including the average vertical velocity within a core $\overline{w}$, the extreme vertical velocity within a core $w_{\max}$, and the intercepted length of a convective core D.

The computed core statistics are individually sorted and the median values and the 10% values are reported.

From Figure 4a, core diameters are quite small, and change little with height. The median values of updraft core diameter are typically between 1 and 1.5 km, with the 10% value typically between 2 and 2.5 km. For downdraft cores, the corresponding values are 1 km and 1.5 - 2.5 km, respectively. These values are close to the results of the previous observational studies, which show the median values for convective core diameter are around 1 km, with typical 10% updraft core diameters between 1.5 and 4 km and 10% downdraft core diameters between 1 and 2.5 km. Vertical velocities in updraft cores increase with height from the minimum values at the lowest level to the maximum values between 3.5 and 5.5 km (near the 0°C level). The median values of maximum vertical velocity in updraft cores are typically between 1.6 and 3.8 m s^{-1}, with 10% value between 2.5 and 8.5 m s^{-1} (Figure 4b). These values are a little smaller than those from observational studies, 2 - 4.5 m s^{-1} and 3 - 10 m s^{-1}, respectively. The median and 10% values of average vertical velocity in updraft cores are separately 1.5 - 2.5 m s^{-1} and 2 - 5.3 m s^{-1} (Figure 4c), which are pretty close to the corresponding observed values, 1.5 - 2.5 m s^{-1} and 2.5-5.5 m s^{-1}. For downdrafts, the change of speed with height is rather modest. The 10% and median values of maximum downward speeds are 2.3 - 3.4 m s^{-1} and 1.5 - 2 m s^{-1} respectively, with the corresponding values for average speeds between 1.6 and 2.5 m s^{-1}, and between 1.2 and 1.6 m s^{-1}. These values are a little smaller than those observed from previous observational studies, with the 10% and median average speeds 2 - 3 m s^{-1} and 1.5 - 2 m s^{-1}, the 10% and median maximum downdraft velocities 2.5 - 6 m s^{-1} and 2 - 3 m s^{-1}. From the above analysis, the simulated speeds of updraft and downdraft cores compare rather closely with those obtained from previous observational studies of vertical motions in deep convective oceanic cloud systems. Because the simulated vertical velocity statistics of KWAJEX precipitating systems are close to those observed in other tropical ocean regions it seems appropriate to consider the KWAJEX simulation

as representative of large tropical ocean MCSs, at least to the first order. The 3-D University of Utah Cloud-Resolving model captures the main dynamic characteristics of this deep MCS over Kwajalein.

b. Simulated precipitation features

In this study, based on the contour plots of convolved simulated 85-GHz brightness temperature and radar reflectivity, the simulated precipitation features are defined in a way that is consistent with the way used to analyze the TRMM data in Nesbitt et al. (2000), i.e., an area is required to be 300 or more contiguous grids in size (area $\geq$ 75 km^2) and to contain either a near-surface reflectivity > 20 dBZ or an 85 GHz PCT < 250 K. For the total of 49 snapshots (a 15 minute output frequency) during the 12-hour simulation period, there are 66 precipitation features, 35 of which are satisfy the criteria for PF with MCS in Nesbitt et al. (2000).

The intensities of the simulated precipitation features, the cumulative distribution functions of minimum 85- and 37-GHz PCT, maximum height of the 20- and 40-dBZ echo, and maximum 6- and 9-km reflectivity, are analyzed and compared to the corresponding statistical results of the TRMM observation in the region of Kwajalein (Figure 5). Compared to TRMM observed values, the simulated 37-GHz PCTs are lower and simulated maximum height of the 20- and 40-dBZ echo and maximum 6- and 9-km reflectivity are higher. For minimum 85-GHz PCT, the simulated precipitation features with ice scattering are very close to the observations, and the simulated features with MCSs have 85 GHz brightness temperatures only 10-20 K higher than those of the TRMM statistics. The simulation's minimum 37-GHz PCT are much lower than the observations, especially for the features with MCS, which are 10-40 K lower (Figure 5b). The model overestimates the maximum height of the 20-dBZ echo for the features with ice scattering, while the simulated values are very close to the observations for the features with MCS (Figure 5c). Figure 5d shows that the model overestimates the maximum height of the 40-dBZ echo for

the features with MCS by 1-3 km. Similarly, the simulation overestimates the maximum reflectivity at 6- and 9-km (Figure 5e, f). The simulated features with MCS have 4-5 dBZ higher echoes at 6 km than the TRMM observations, with 8-10 dBZ higher echoes at 9 km than the TRMM statistics.

From the analysis in section 2, the observed 11-12 August 1999 precipitating system is weak-to-average in terms of "proxies" for convective intensity - radar reflectivity and brightness temperature, against the 5-year TRMM sampled 108 MCSs in the region of Kwajalein. Therefore, except for the minimum 85-GHz PCT, other simulated TRMM parameters are more extreme than the statistically-likely actual values. The minimum 37-GHz PCT, maximum height of the 40-dBZ echo, and maximum reflectivity at 9 km, which are all sensitive to larger ice particles, are more extreme than the minimum 85-GHz PCT, maximum height of the 20-dBZ echo, and maximum reflectivity at 6 km, respectively, which are not as sensitive to larger ice particles. This implies that the bulk microphysics scheme is producing large ice particles at mid- to upper levels that are too numerous.

c. Comparison of simulated reflectivities to ground radar observations

The CCFAD of echo observed by the Kwajalein ground S-band radar for the 11-12 August 1999 convective system is analyzed in section 2. In order to compare the simulated system to the observations, the frequency distribution of simulated radar reflectivity with height is analyzed (Figure 6). This CCFAD from the simulation is accumulated from 2025 UTC 11 August to 0200 UTC 12 August 1999 every 5 minutes for the whole model domain, with a constant bin size of 1 dBZ. In this study, only the columns with the 1.5-km reflectivity greater than or equal to 20 dBZ are selected for statistical analysis, which makes it consistent with the criterion for the Kwajalein ground S-band radar reflectivity statistics. This eliminates about a fifth of the samples that were originally present without this restriction. The total number of columns that fulfill the

selection criteria is 899016.

The overall pattern in the CCFAD (Figure 6a) resembles that for the ground radar observation statistics (Figure 2). Reflectivity increases with decreasing height. The median near-surface reflectivity is 29 dBZ, which is equal to the corresponding value for radar observation statistics. The top 10% near-surface reflectivity is 39 dBZ, very close to the radar observed value. The top 1% quantile has reflectivity of 43 dBZ at the near surface level, equal to that for the radar observation. The quantitative differences between model simulation and radar observation statistics (Figure 6b) indicate that the differences are less than 2 dBZ at the levels below 5 km. Above 6 km, the differences increase with height and reach a maximum at around 9 km. The simulated radar reflectivities are statistically 5-13 dBZ higher than those from radar observation at the levels between 7 and 10.5 km, where graupel is the dominant ice species. Therefore, an anomalously large graupel mixing ratio that is associated with too many large graupel particles based on the assumed exponential size distribution, is quite possibly the reason for the anomalously high simulated radar reflectivity.

Frequency distributions of both the radar observed and model simulated reflectivity at 1.5-, 6-, 9- and 12-km are shown in Figure 7 (bin size is 2 dBZ for this figure). At 1.5 km, the radar reflectivity is attributed to rain water and the model simulation results are very close to the radar observations. *At higher levels, the model tends to overpredict the radar reflectivity.* At 6 km, the simulated reflectivity is generally 4-5 dBZ larger than that observed. The simulated maximum reflectivity at 6 km is approximately 44 dBZ, which is larger than the maximum reflectivity of 40 dBZ observed by the Kwajalein ground-based radar. At 9 km, the simulated reflectivity (40 dBZ) is much larger than was observed (28 dBZ). At 12 km, the model overpredicts the frequency of occurrence of reflectivity greater than about 10 dBZ. The simulated maximum reflectivity at 12 km is approximately 28 dBZ, which is larger than the maximum reflectivity of about 18 dBZ observed by the radar.

d. Comparison of simulated graupel mixing ratio to in situ observations

For the MCS of 11-12 August 1999, the best cloud microphysics data come from University of North Dakota Citation (Stith et al. 2002). The Citation was repeatedly directed toward the strongest echoes of the convective portion of the storm system, during the time when the MCS was at its most intense phase. The NASA DC8 didn't collect much data on that day due to instrument and aircraft icing problems. From the "common microphysics product" (Kingsmill et al. 2004) for KWAJEX, the Citation flew and collected data for about 3.5 h (2200 UTC 11 August – 0131 UTC 12 August 1999). The time series of Citation temperature and ice water content for the mission are shown in Figure 8a. Mean Citation temperature was about -4 °C (with a range of 8 to -17 °C, corresponding to an altitude range of 3 – 7.3 km). The ice water content varied greatly during the mission. During the 22-min period of 2202 – 2224 UTC (indicated by A-B in Figure 8a), the Citation flew at a constant temperature and height (about -10°C and 6.4 km) within a strong convective area. The observed total ice water mixing ratio during this period reaches a maximum of about 4 g kg^{-1} in several cores (Figure 8b). It is not yet possible to distinguish the contributions made by the different ice species on this flight, but we can show that the simulated graupel content alone exceeds the total ice water content that was observed.

Figure 9 shows the histogram of model simulated graupel mixing ratio for cloudy (saturated) grid points at 6.4 km during 2100-2300 UTC. The bin size employed for this histogram is 0.2 g kg^{-1}. Cloudy (saturated) grid is defined as a grid point with $q_c + q_i > 0.01 \times q_{sat}$ (q_{sat} is the saturation mixing ratio over liquid water at that point). During 2100-2300 UTC, there are 246777 cloudy grid points identified from the total of 416025 model grid points at 6.4 km. About 0.5% of these grid points, nearly 500 points in all, have graupel mixing ratios greater than 4 g kg^{-1}, or the highest values of measured total ice water mixing ratio. This alone would support

a finding that convective-scale peaks of graupel content are likely overestimated by the model at that level. If the contribution of graupel to total ice water content is less than 50%, as is commonly believed, this conclusion would be strengthened.[1] According to the assumed exponential size distributions for graupel particle, it can be concluded that the maximum graupel size is also likely to be overestimated at that level. From the comparison of model simulated to radar observed reflectivity, the biggest differences are at around 9 km. Unfortunately, no appropriate in situ microphysics observations are available near the 9 km level for this case.

5. Conclusion

The 3-D University of Utah Cloud-Resolving model has been employed to simulate the large mesoscale precipitation system of 11-12 August 1999, which is the best-sampled large system during KWAJEX. The analysis of a contoured cumulative frequency by altitude diagram of radar reflectivity shows that this system, compared with the 5-year TRMM observation statistics for the Kwajalein area, is large in size, and weak-to-average in proxies of convective intensity. Comparing the TRMM statistics for the Kwajalein area with those sampled by aircraft (GATE, near Australia, TOGA COARE; not shown), Kwajalein has a smaller percentage of such large MCSs, but the TRMM-observed proxies for convective intensity for these large MCSs vary rather little across these four regions, and indeed over most of the tropical oceans.

From the model simulation results, convective cores are identified and analyzed using the methodology similar to that used for aircraft observational sampling of cores in GATE, oceans near Tropical Australia, and the Western Pacific. The computation of the median and 10% values of average, maximum vertical velocity within the simulated cores and the diameters of the cores indicates that the model simulation values compare favorably with those obtained from previous observational studies of oceanic vertical motions.

The TRMM precipitation feature database provides observational constraints on cloud

system properties. Based on the simulated 85-GHz brightness temperature and near surface radar reflectivity, the precipitation features are defined in a way that is consistent with the way used to analyze the TRMM data in Nesbitt et al. (2000). During the 12-h simulation period, 66 precipitation features were identified, of which 35 met the criteria for a PF with MCS. Comparison of model simulation results to the TRMM observation statistics for the Kwajalein area shows that the model tends to underestimate microwave brightness temperature and overestimate radar reflectivity, especially for those parameters associated with larger ice particles.

The comparison between the reflectivity statistics of the model simulation and those of the KWAJEX ground-based precipitation radar observations indicates that the differences are small and insignificant at levels below 5 km. Above 6 km, the reflectivity differences increase with height and reach a maximum at around 9 km. The simulated radar reflectivities are statistically 5-13 dBZ higher than those from radar observation at levels between 7 and 10.5 km, where graupel is the dominant simulated ice species. Simulated graupel mixing ratios as large as 8 g kg^{-1} are quite possibly the reason for the unrealistically high simulated radar reflectivity. Comparison of model simulated graupel mixing ratio with in situ microphysics observations from the Citation indicates that the model overestimates graupel content at the level the Citation flew (about 6.4 km).

Therefore, a question arises: what contributes to these unrealistically high simulated graupel mixing ratios? Is it deficiencies in the microphysics parameterization, overprediction of convective vertical velocity, or both? The analysis of simulated convective cores in this study indicates that the simulated vertical velocities compare favorably with those obtained from previous observational studies of oceanic vertical motions, in regions where TRMM-observed proxies in such systems are similar. Therefore, we suggest that the simulated vertical velocities are realistic and probably not the primary reason for the unrealistically high graupel contents. It then follows that deficiencies in the microphysics parameterization are more likely to be the

source of the overprediction of graupel and radar reflectivity. The bulk microphysics scheme overestimates the ice water content, especially of large particles at mid- to upper levels. This result is consistent with those from several previous studies (e.g., Tao et al. 2003; Wiedner et al. 2004; McFarquhar et al. 2006; Lang et al. 2007) that found that bulk microphysics schemes tend to overestimate graupel in numerical simulations.

Graupel plays an important role in this simulation because conversion processes of graupel are a significant component of latent heat release, which in turn has a significant impact on the dynamic, thermodynamic, and precipitation characteristics of the evolving MCS. Also, the greater fall speed of graupel compared to low-density ice particles allows graupel to remain suspended in strong updrafts longer, and to fall out of weak updrafts faster. In order to simulate convective clouds accurately, it is important to represent all species conversion processes for graupel as realistically as possible. However, many CRMs that use bulk microphysics schemes tend to overpredict graupel. In Part II of this study, the bulk microphysical processes associated with graupel production in this large MCS are examined in detail to indicate the relative contribution of accretion of supercooled cloud water, supercooled rain, and snow.

The bulk microphysics scheme used in this study contains a range of assumptions about such factors as the density and size distribution intercept of precipitating hydrometeors, number concentration or riming processes. It has been indicated that many simulated convective characteristics are more strongly influenced by differences in size distribution intercept parameter and particle density than by differences in the way that microphysical processes are treated in the ice schemes (McCumber et al. 1991). Such microphysical parameters vary greatly from case to case, or even in the same convective system (e.g., Brown and Swann 1997; McFarquhar and Black 2004). The current version of the microphysics scheme employed in this study uses fixed values of the intercept parameters N_0 and density for graupel particles, which may have significant effects on the simulated graupel production. In Part II of this study, a set of numerical

simulations of the KWAJEX 11-12 August 1999 MCS, using different intercepts for the number concentration of graupel, and different graupel densities to investigate the roles of such parameters in the simulated convective vertical velocity, water/ice mixing ratio and bulk microphysical processes associated with graupel production, will be described.

In this study, we simulated and analyzed the largest MCS observed during KWAJEX. Future work would expand the simulation and analysis from one MCS case to other cases. Future cloud-resolving model simulations should be conducted to study other cloud regimes.

Footnote 1: As of this writing, there is work in progress that is likely to demonstrate that the maximum contribution of graupel to the ice water content is *considerably* less than 50% (David Kingsmill, personal communication), specifically including the flight in the 11-12 August MCS. Experience in hurricanes, arguably analogous to large oceanic MCSs microphysically, also indicates that graupel fractions of ice water content are less than 50% (Robert A. Black, personal communication). It is indeed unfortunate that there are so few quantitative measurements of ice microphysical properties over tropical oceans in the -10 to -40 ˚C temperature range.

Acknowledgements. The authors would like to thank Dr. Greg McFarquhar, Dr. Zhaoxia Pu, Dr. Jay Mace, Dr. Peter Blossey, Dr. Marat Khairoutdinov, Dr. Wojciech Grabowski, Dr. Chuntao Liu, Dr. Ruiyu Sun, Dr. Steve Nesbitt and Dr. Haiyan Jiang for their discussion, comments and suggestions. Thanks are also extended to Dr. Sandra Yuter for providing Kwajalein ground-based radar data, Dr. Chris Kummerow for providing the microwave radiative transfer model, and Dr. David Kingsmill for providing Citation data and his comments on microphysics data. This study is partially funded by NASA Grant NAG5-10682 (TRMM and hurricane research) supported by Ramesh Kakar, by NASA Grant NAG5-11504, and by the National Science Foundation Science and Technology Center for Multi-Scale Modeling of

Atmospheric Processes, managed by Colorado State University under cooperative agreement No. ATM-0425247. We also appreciate the constructive comments by three anonymous reviewers.

References

Beesley, T. A., C. S. Bretherton, C. Jakob, E. L. Andreas, J. M. Intrieri, and T. A. Uttal, 2000: A comparison of cloud and boundary layer variables in the ECMWF forecast model with observations at Surface Heat Budget of the Arctic Ocean (SHEBA) ice camp. *J. Geophys. Res.*, **105**, 12337-12349.

Blossey, P. N., C. S. Bretherton, J. Cetrone and M. Khairoutdinov, 2007: Cloud-resolving model simulations of KWAJEX: Model sensitivities and comparisons with satellite and radar observations. *J. Atmos. Sci.,* **64,** 1488-1508.

Brown, P. R., and H. A. Swann, 1997: Evaluation of key microphysical parameters in three-dimensional cloud-model simulations using aircraft and multiparameter radar data. *Quart. J. Roy. Meteor. Soc.,* **123**, 2245–2275.

Chaboureau, J.-P., J.-P. Cammas, P. Mascart, J.-P. Pinty, C. Claud, R. Roca, and J.-J. Morcrette, 2000: Evaluation of a cloud system life-cycle simulated by Meso-NH model during FASTEX using METEOSAT radiances and TOVS-3I cloud retrievals. *Quart. J. Roy. Meteor. Soc.,* **126**, 1735–1750.

_____, _____, _____, and _____, 2002: Mesoscale model cloud scheme assessment using satellite observations. *J. Geophys. Res.,* **107**, doi:10.1029/2001JD000714.

Cetrone, J. and R. A. Houze Jr., 2006: Characteristics of Tropical Convection over the Ocean near Kwajalein. *Mon. Wea. Rev.,* **134**, 834–853.

Deardorff, J. W., 1980: Stratocumulus-capped mixed layers derived from a three-dimensional model. *Bound.-Layer. Meteor.*, **18**, 495-527.

Ferrier, B. S., 1994: A double-moment multiple-phase four-class bulk ice scheme. Part I: Description. *J. Atmos. Sci.,* **51**, 249–280.

_____, 2003: Cloud microphysics modeling: the lasting legacy of Harorld D. Orville. *Harold D. Orville Symposium Program,* Rapid City, SD, April 26. [Available online at:

http://www.ias.sdsmt.edu/Orville%20Symposium/Abstracts/Ferrier.pdf]

Fu Q., and K. N. Liou, 1993: Parameterization of the radiative properties of clouds. *J. Atmos. Sci.*, **50**, 2008–2025.

_____, S. K. Krueger, and K. N. Liou, 1995: Interactions of radiation and convection in simulated tropical cloud clusters. *J. Atmos. Sci.*, **52**, 1310–1328.

Garrett, T. J., M. A. Zulauf, and S. K. Krueger, 2006: Effects of cirrus near the tropopause on anvil cirrus dynamics, *Geophys. Res. Lett,* 33, L17804, doi:10.1029/2006GL027071.

Grabowski, W. W., X. Wu, M. W. Moncrieff, and W. D. Hall, 1999: Cloud resolving modeling of topical cloud systems during Phase III of GATE. Part III: Effects of cloud microphysics. *J. Atmos. Sci.,* **56**, 2384-2402.

Hall, W. D, 1980: A detailed microphysical model within a two-dimensional dynamic framework: Model description and preliminary results. *J. Atmos. Sci.,* **37**, 2486–2507.

Johnson, D., W.-K. Tao, J. Simpson, and C.-H. Sui, 2002: A study of the response of deep tropical clouds to large-scale processes, Part I: Model set-up strategy and comparison with observation, *J. Atmos. Sci.*. 59, 3492-3518.

Jorgensen, D. P., E. J. Zipser and M. A. LeMone. 1985: Vertical Motions in Intense Hurricanes. *J. Atmos. Sci*., **42**, 839–856.

_____ and M. A. LeMone. 1989: Vertically Velocity Characteristics of Oceanic Convection. *J. Atmos. Sci*., **46**, 621–640.

Khain A. P, I Sednev, and V Khvorostyanov, 1996: Simulation of coastal circulation in the eastern Mediterranean using a spectral microphysics cloud ensemble model. *J. Climate*, **9**, 3298–3316.

_____, A Pokrovsky, and I Sednev, 1999: Effects of cloud-aerosol interaction on cloud-microphysics, precipitation formation and size distribution of atmospheric aerosol: Numerical experiments with a spectral microphysics cloud model. *Atmos. Res*, **52**, 195–220.

_____, M Ovtchinnikov, M Pinsky, A Pokrovsky, and H Krugliak, 2000: Notes on the state-of-the art numerical modeling of cloud microphysics. *Atmos. Res*, **55**, 159–224.

_____, D Rosenfeld, and A Pokrovsky, 2001: Simulating convective clouds with sustained supercooled liquid water down to −37.5°C using a spectral microphysics model. *Geophys. Res. Lett*, **28**, 3887–3890.

_____, A Pokrovsky, M Pinsky, A Seifert, and V Phillips, 2004: Simulation of effects of atmospheric aerosols on deep turbulent convective clouds by using a spectral microphysics mixed-phase cumulus cloud model. Part I: Model description and possible applications. *J. Atmos. Sci*, **61**, 2963–2892.

Khairoutdinov, M. F., and D. A. Randall, 2003: Cloud resolving modeling of the ARM summer 1997 IOP: model formulation, results, uncertainties, and sensitivities. *J. Atmos. Sci*., **60**, 607-625.

Kingsmill, D. E., and coauthors, 2004: TRMM common microphysics products: A tool for evaluating spaceborne precipitation retrieval algorithms. *J. Appl. Meteror*., **43**, 1598-1618.

Krueger, S. K., Q. Fu, K. N. Liou, and H-N. S. Chin, 1995: Improvements of an ice-phase microphysics parameterization for use in numerical simulations of tropical convection. *J. Appl. Meteror*., **34**, 281-287.

_____, and Y.-L. Luo, 2007: Cloud Properties Simulated by a Single-Column Model. Part III: Radiative Effects of Cloud Types and Comparison with Satellite Observations and Results from a Cloud-Resolving Model. To be submitted to *J. Atmos. Sci.*

Kummerow, C., and J. A. Weinman, 1988: Determining microwave brightness temperatures from horizontally finite, vertically structured clouds. *J. Geophys. Res.*, **93**, 3720-3728.

LeMone, M. A., and E. J. Zipser, 1980: Cumulonimbus vertical velocity events in GATE. Part I: Diameter, intensity, and mass flux. *J. Atmos. Sci*., **37**, 2444-2457.

Lang, S., W.-K. Tao, R. Cifelli, W. Olson, J. Halverson, S. Rutledge, and J. Simpson, 2007:

Improving simulations of convective system from TRMM LBA: Easterly and Westerly regimes. *J. Atmos. Sci.,* **64**, 1141-1164.

Li, Y.-P., 2003: Intensity of convective storms in Florida and their environmental properties. Master thesis, Department of Meteorology, University of Utah, 123 pp. [Available online at: ftp://ftp.met.utah.edu/pub/ezipser/yaping/thesis/thesis_li.pdf]

_____, 2006: Cloud resolving simulations of tropical cloud systems: using field program observations to evaluate ice phase microphysics parameterizations. Ph.D. dissertation, Department of Meteorology, University of Utah, 184 pp. [Available online at: ftp://ftp.met.utah.edu/pub/ezipser/yaping/thesis/dissertation_li.pdf]

Lin, Y. L., R. D. Farley, and H. D. Orville, 1983: Bulk parameterization of the snow field in a cloud model. *J. Climate Appl. Meteor.*, **22**, 1065-1092.

Lord, S. J., H. E. Willoughby and J. M. Piotrowicz, 1984: Role of a parameterized ice-phase microphysics in an axisymmetric tropical cyclone model. *J. Atmos. Sci.,* **41**, 2836–2848.

Lucas, C., M. A. Lemone, and E. J. Zipser, 1994: Vertical Velocity in Oceanic Convection off Tropical Australia. *J. Atmos. Sci.,* **51**, 3183–3193.

Luo, Y.-L., S. K. Krueger, G. G. Mace, and K.-M. Xu, 2003: Cirrus cloud statistics from a cloud-resolving model simulation compared to cloud radar observations. *J. Atmos. Sci.,* **60**, 510–525.

Lynn, B. H., A. P. Khain, J. Dudhia, D. Rosenfeld, A. Pokrovsky and A. Seifert. 2005: Spectral (Bin) Microphysics Coupled with a Mesoscale Model (MM5). Part I: Model Description and First Results. *Mon. Wea. Rev.*, **133**, 44–58.

Marshall, J. S., and W. M. Palmer, 1948: The distribution of raindrops with size. *J. Meteor.*, **5**, 165-166.

Nesbitt, S. W., E. J. Zipser, and D. J. Cecil, 2000: A census of precipitation features in the Tropics using TRMM: Radar, ice scattering, and lightning observations. *J. Climate*, **13**, 4087-

4106.

McCumber, M., W. K. Tao, J. Simpson, R. Penc, and S. T. Soong, 1991: Comparison of ice-phase microphysical parameterization schemes using numerical simulations of convection. *J. Appl. Meteor*., **30**, 708-721.

McFarquhar, G. M and R. A. Black, 2004: Observations of particle size and phase in tropical cyclones: Implications for mesoscale modeling of microphysical processes. *J. Atmos. Sci.,* **61**, 422–439.

_____, H. Zhang, G. Heymsfield, R. Hood, J. Dudhia, J. B. Halverson, and F. Marks Jr., 2006: Factors affecting the evolution of hurricane Erin (2001) and the distribution of hydrometeors: Role of microphysical processes. *J. Atmos. Sci.,* **63**, 127–150.

Meyers, M. P., R. L. Walko, J. Y. Harrington, and W. R. Cotton, 1997: New RAMS cloud microphysics parameterization. Part II: The two-moment scheme. *Atmos. Res.,* **45**, 3–39.

Milbrandt, J. A., and M. K. Yau, 2005: A multimoment bulk microphysics parameterization. Part II: A proposed three-moment closure and scheme description. *J. Atmos. Sci.,* **62**, 3065–3081.

Morrison, H., J. A. Curry and V. I. Khvorostyanov, 2005: A New Double-Moment Microphysics Parameterization for Application in Cloud and Climate Models. Part I: Description. *J. Atmos. Sci.,* **62**, 1665–1677.

Ovtchinnikov, M, and Y. I Kogan, 2000: An investigation of ice production mechanisms in small cumuliform clouds using a 3D model with explicit microphysics. Part I: Model description. *J. Atmos. Sci.,* **57**, 3004–3020.

Prasad, N., H.-Y. M. Yeh, R. F. Adler and W.-K. Tao, 1995: Infrared and microwave simulations of an intense convective system and comparison with aircraft observations, *J. Appl. Meteor*., **34**, 153-174.

Reisner, J., R. M. Rasmussen, and R. T. Bruintjes, 1998: Explicit forecasting of supercooled liquid water in winter storms using the MM5 forecast model. *Quart. J. Roy. Meteor. Soc.,*

124, 1071–1107.

Rutledge S. A, and P. V Hobbs, 1984: The mesoscale and microscale structure and organization of clouds and precipitation in midlatitude cyclones. Part XII: A diagnostic modeling study of precipitation development in narrow cold-frontal rainbands. *J. Atmos. Sci*, **41**, 2949–2972.

Simpson, J., C. Kummerow, W.-K. Tao and R. Adler, 1996: On the Tropical Rainfall Measuring Mission (TRMM) *Meteor, and Atmos. Phys.* 60, 19-36.

Schultz P, 1995: An explicit cloud physics parameterization for operational numerical weather prediction. *Mon. Wea. Rev*, **123**, 3331–3343.

Smith, P. L., Jr., C. G. Myers and H. D. Orville, 1975: Radar reflectivity factor calculations in numerical cloud models using bulk parameterization of precipitation. *J. Appl. Meteor.*, **14**, 1156-1165.

_____, 1984: Equivalent radar reflectivity factors for snow and ice particles. *J. Climate Appl. Meteor.*, **23**, 1258-1260.

Sobel, A. H., S. E. Yuter, C. S. Bretherton, and G. N. Kiladis, 2004: Large-scale meteorology and deep convection during TRMM KWAJEX. *Mon. Wea. Rev.,* **132**, 422–444.

Soong, S.-T., and Y. Ogura, 1980: Response of trade wind cumuli to large-scale processes. *J. Atmos. Sci.,* **37,** 2035–2050.

_____, and W.-K. Tao, 1980: Response of deep tropical clouds to mesoscale processes. *J. Atmos. Sci.,* **37,** 2016–2036.

Spencer, R. W., H. M. Goodman, and R. E. Hood, 1989: Precipiation retrieval over land and ocean with the SSM/I: Identification and characteristics of the scattering signal. *J. Atmos. Oceanic. Technol*., **6**, 254-273.

Spooner, C. L., 2001: Dual-Doppler analysis of an oceanic tropical mesoscale system during the Kwajalein Experiment (KWAJEX). M.S. thesis, Atmospheric Sciences Group, Texas Tech University, 112 pp.

Stevens, D. E., and C. S. Bretherton, 1996: A new forward-in-time advection scheme and adaptive multilevel flow solver for nearly incompressible atmospheric flow. *J. Comput. Phys.*, **129**, 284-295.

Stith, J. L., J. E. Dye, A. Bansemer, A. J. Heymsfield, C. A. Grainger, W. A. Petersen, and R. Cifelli, 2002: Microphysical observations of tropical clouds. *J. Appl. Meteor.,* **41**, 97–117.

Tao W.-K, Coauthors, 2003: Microphysics, radiation and surface processes in a non-hydrostatic model. *Meteor. Atmos. Phys*, **82**, 97–137.

Toracinta, E. R., D. J. Cecil, E. J. Zipser, and S. W. Nesbitt, 2002: Radar, passive microwave, and lightning characteristics of precipitating systems in the Tropics. *Mon. Wea. Rev*. **130**, 802-824.

Wang, Y., 2002: An explicit simulation of tropical cyclones with a triply nested movable mesh primitive equation model—TCM3. Part II: Model refinements and sensitivity to cloud microphysics parameterization. *Mon. Wea. Rev.,* **130**, 3022–3036.

Wicker, L. J., and W. C. Skamarock, 1998: A time-splitting scheme for the elastic equations incorporating second-order Runge-Kutta time differencing. *Mon. Wea. Rev*., **126**, 1992-1999.

Wiedner, M., C. Prigent, J. R. Pardo, O. Nuissier, J. Chaboureau, J. Pinty, and P. Mascart, 2004: Modeling of passive microwave responses in convective situations using output from mesoscale models: Comparison with TRMM/TMI satellite observations. *J. Geophys. Res.*, **109**, D06214, doi:10.1029/2003JD004280.

Xu, K.-M., and Coauthors, 2002: An intercomparison of cloud-resolving models with the ARM summer 1997 IOP data. *Quart. J. Roy. Meteor. Soc.*, **128**, 593-624.

Yeh, H.-Y. M., N. Prasad, R. Meneghini, W.-K. Tao and R. F. Adler, 1995: Model-based simulation of TRMM spaceborne radar observations, *J. Appl. Meteor.,* **34**, 175-197.

Yuter, S. E., R. A. Houze Jr., E. A. Smith, T. T. Wilheit, and E. J. Zisper, 2005: Pyhsical characterization of tropical oceanic convection observed in KWAJEX. *J. Appl. Meteor*., **44**,

385-415.

Zalesak, S. T., 1979: Fully multidimensional flux-corrected transport. *J. Comput. Phys.*, **31**, 335-362.

Zhang, M. H., J. L. Lin, R. T. Cederwall, J. J. Yio, and S. C. Xie, 2001: Objective analysis of ARM IOP data: Method and sensitivity. *Mon. Wea. Rev.,* **129**, 295–311.

_____ 2003. Variational objective analysis of the TRMM KWAJEX IOP data. Version 1, available at ftp://atmgcm.msrc.sunysb.edu/pub/trmm/kwjx/.

Zipser, E. J., and M. A. LeMone, 1980: Cumulonimbus vertical velocity events in GATE. Part II: Synthesis and model core structure. *J. Atmos. Sci.*, **37**, 2458-2469.

Zulauf, M. A., 2001: Modeling the effects of boundary layer circulations generated by cumulus convection and leads on large-scale surface fluxes. Ph.D. dissertation, Department of Meteorology, University of Utah, 177pp. [Available online at: http://www.met.utah.edu/skrueger/homepages/mazulauf/files/zulauf_thesis_final.pdf]

Figure Captions

Figure 1. CDFs of (a) minimum 85-GHz PCT; (b) minimum 37-GHz PCT; (c) maximum height of the 20 dBZ echo; (d) maximum height of the 40 dBZ; (e) maximum 6-km reflectivity; (f) maximum 9-km reflectivity for TRMM observed precipitation features with MCS in the region of Kwajalein.

Figure 2. CCFADs for the observed Kwajalein ground S-band radar reflectivities during 2024 UTC 11 August to 0200 UTC 12 August 1999. Cumulative frequencies of a 10% quantile from 10-90%, 99%, 99.9%, and 99.99% are contoured; the 50% profile is the solid, thick line.

Figure 3. Numbers of the cloud resolving model simulated updraft and downdraft cores during 1800 UTC August 11 to 0600 UTC August 12 1999.

Figure 4. Variations with altitude of the CRM simulated median (asterisk) and strongest 10% level (Diamond) statistics of (a) diameter, (b) maximum vertical velocity, (c) average vertical velocity during 1800 UTC August 11 to 0600 UTC August 12 1999.

Figure 5. CDFs of (a) minimum 85-GHz PCT; (b) minimum 37-GHz PCT; (c) maximum height of the 20 dBZ echo; (d) maximum height of the 40 dBZ; (e) maximum 6-km reflectivity; (f) maximum 9-km reflectivity for TRMM observed precipitation features in the region of Kwajalein and the CRM simulated PFs during 1800 UTC August 11 to 0600 UTC August 12 1999.

Figure 6. CCFADs for (a) the CRM simulated radar reflectivities during 2025 UTC 11 August to 0200 UTC 12 August 1999; Cumulative frequencies of a 10% quantile from 10-90%, 99%, 99.9%, and 99.99% are contoured; the 50% profile is the solid, thick line. (b) differences between the CRM simulated and the Kwajalein ground radar observed reflectivities for the KWAJEX 11-12 August 1999 precipitating system. Cumulative frequencies are shown as the legend.

Figure 7. PDF of the Kwajalein ground S-band radar observed and the cloud resolving model simulated reflectivities (a) at 1.5 km; (b) 6 km; (c) 9 km; and (d) 12 km during 2025 UTC 11 August to 0200 UTC 12 August 1999.

Figure 8. Time series of (a) Citation temperature and ice water content for the mission between 2200 UTC 11 August and 0131 UTC 12 August 1999 during the KWAJEX; (b) ice water mixing ratio for the 22-min period of 2202 – 2224 UTC [indicated by A-B in (a)] (at ~ 6.4 km).

Figure 9. Histogram of frequency of occurrence of the cloud resolving model simulated graupel mixing ratio for cloudy grid points at 6.4 km during 2100 UTC to 2300 UTC 11 August 1999.

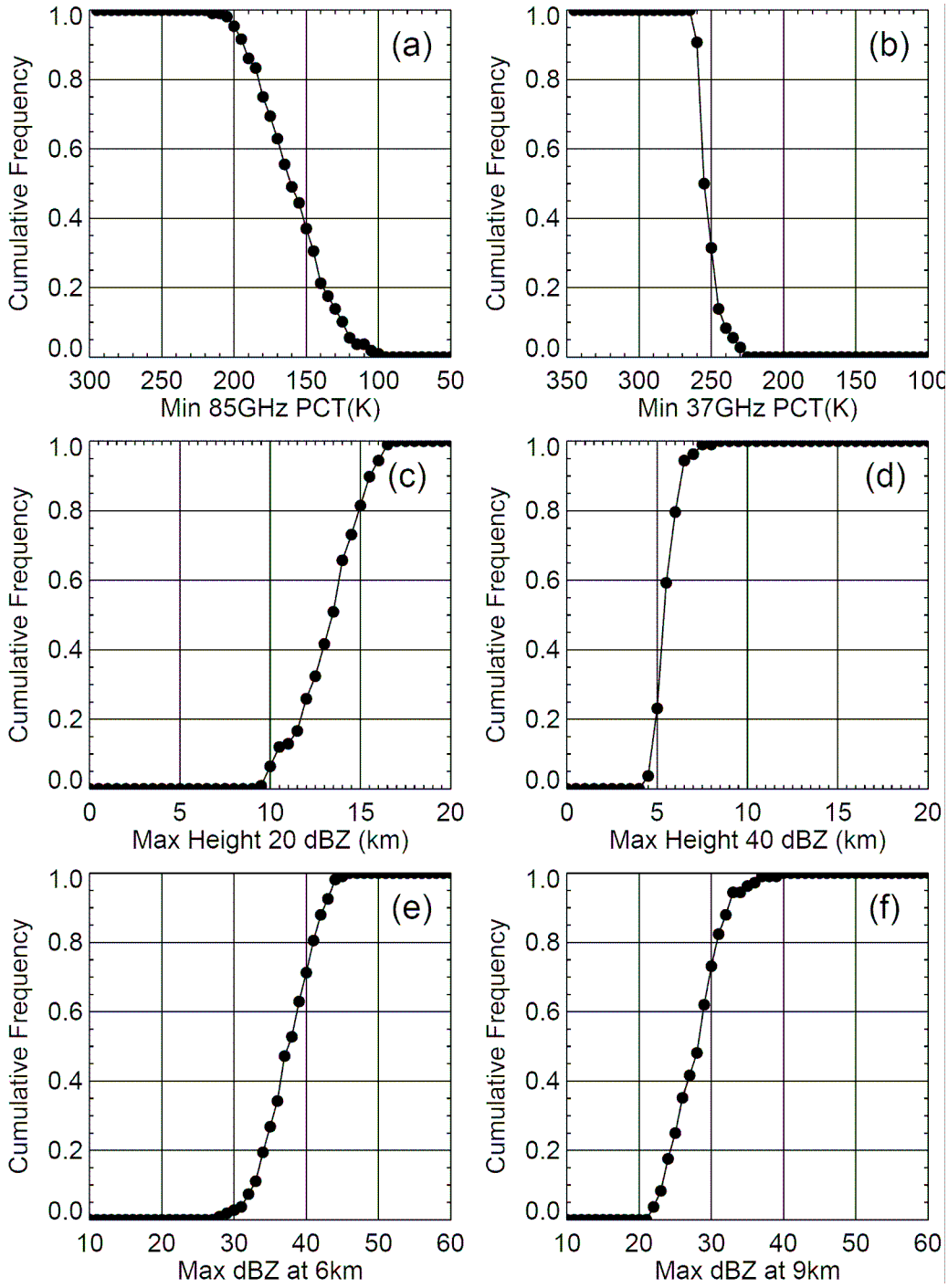

Figure 1. CDFs of (a) minimum 85-GHz PCT; (b) minimum 37-GHz PCT; (c) maximum height of the 20 dBZ echo; (d) maximum height of the 40 dBZ; (e) maximum 6-km reflectivity; (f) maximum 9-km reflectivity for TRMM observed precipitation features with MCS in the region of Kwajalein.

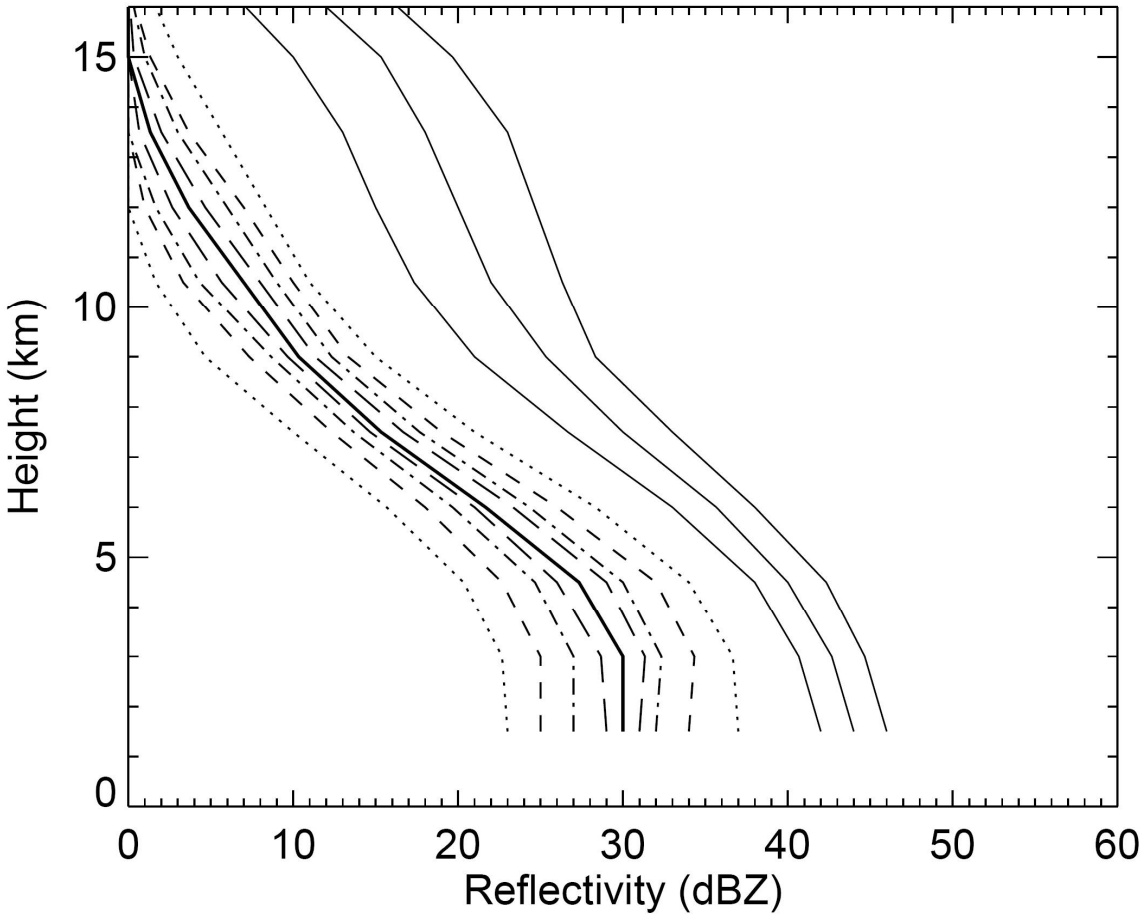

Figure 2. CCFADs for the observed Kwajalein ground S-band radar reflectivities during 2024 UTC 11 August to 0200 UTC 12 August 1999. Cumulative frequencies of a 10% quantile from 10-90%, 99%, 99.9%, and 99.99% are contoured; the 50% profile is the solid, thick line.

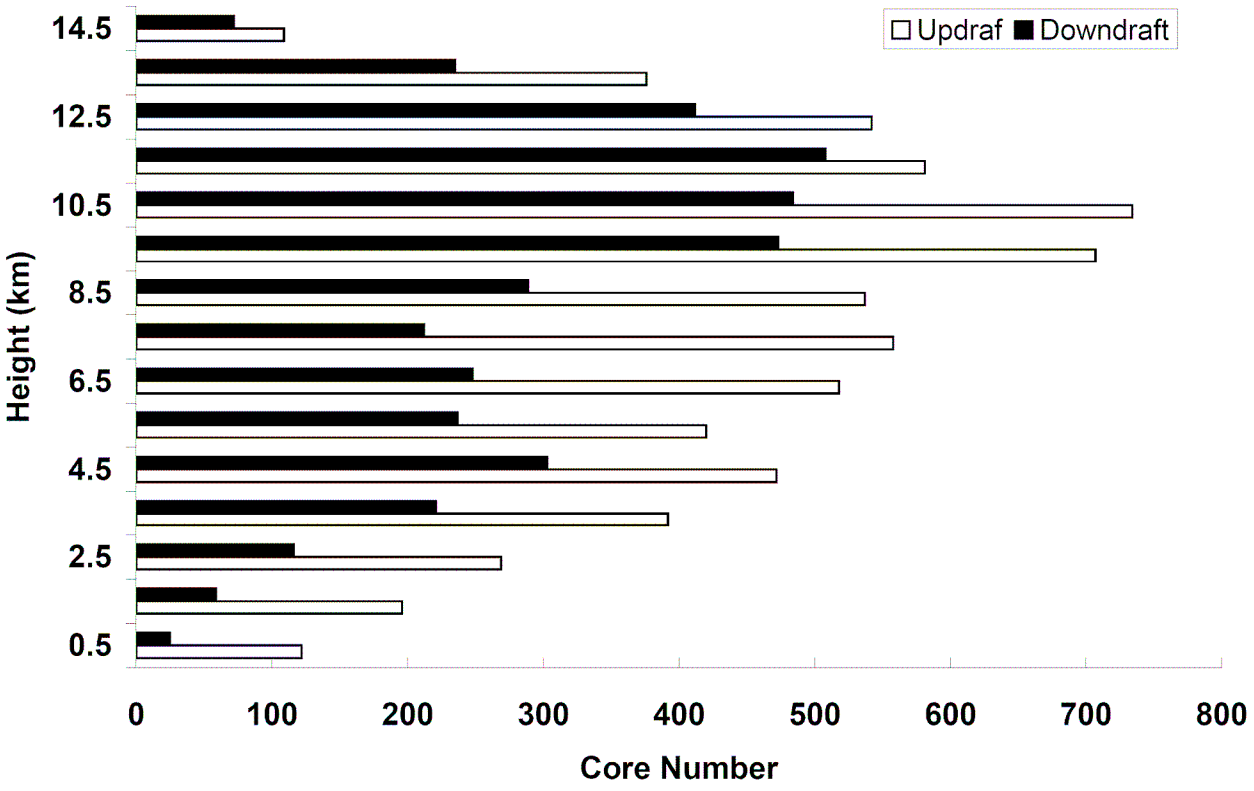

Figure 3. Numbers of the cloud resolving model simulated updraft and downdraft cores during 1800 UTC August 11 to 0600 UTC August 12 1999.

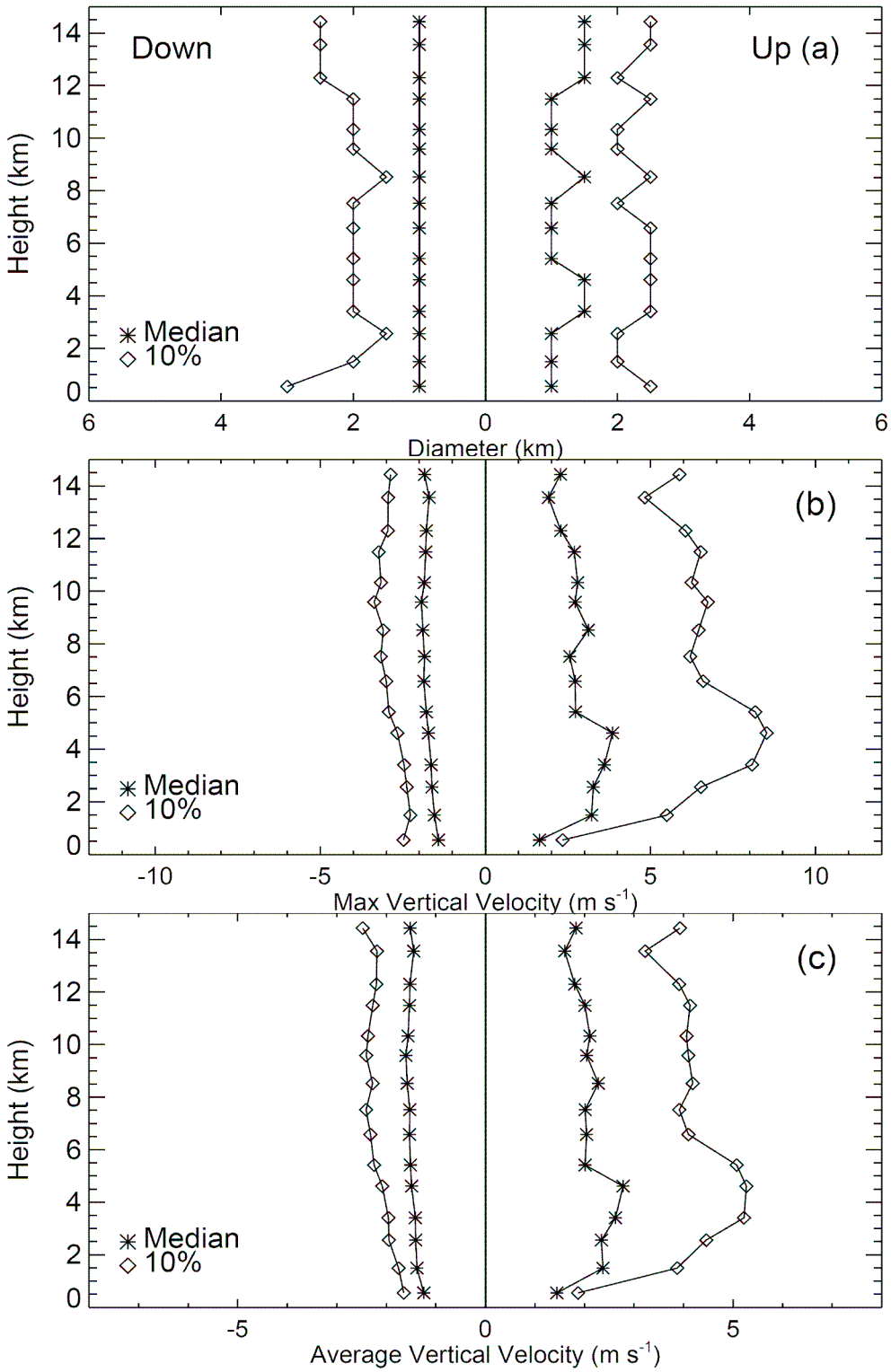

Figure 4. Variations with altitude of the CRM simulated median (asterisk) and strongest 10% level (Diamond) statistics of (a) diameter, (b) maximum vertical velocity, (c) average vertical velocity during 1800 UTC August 11 to 0600 UTC August 12 1999.

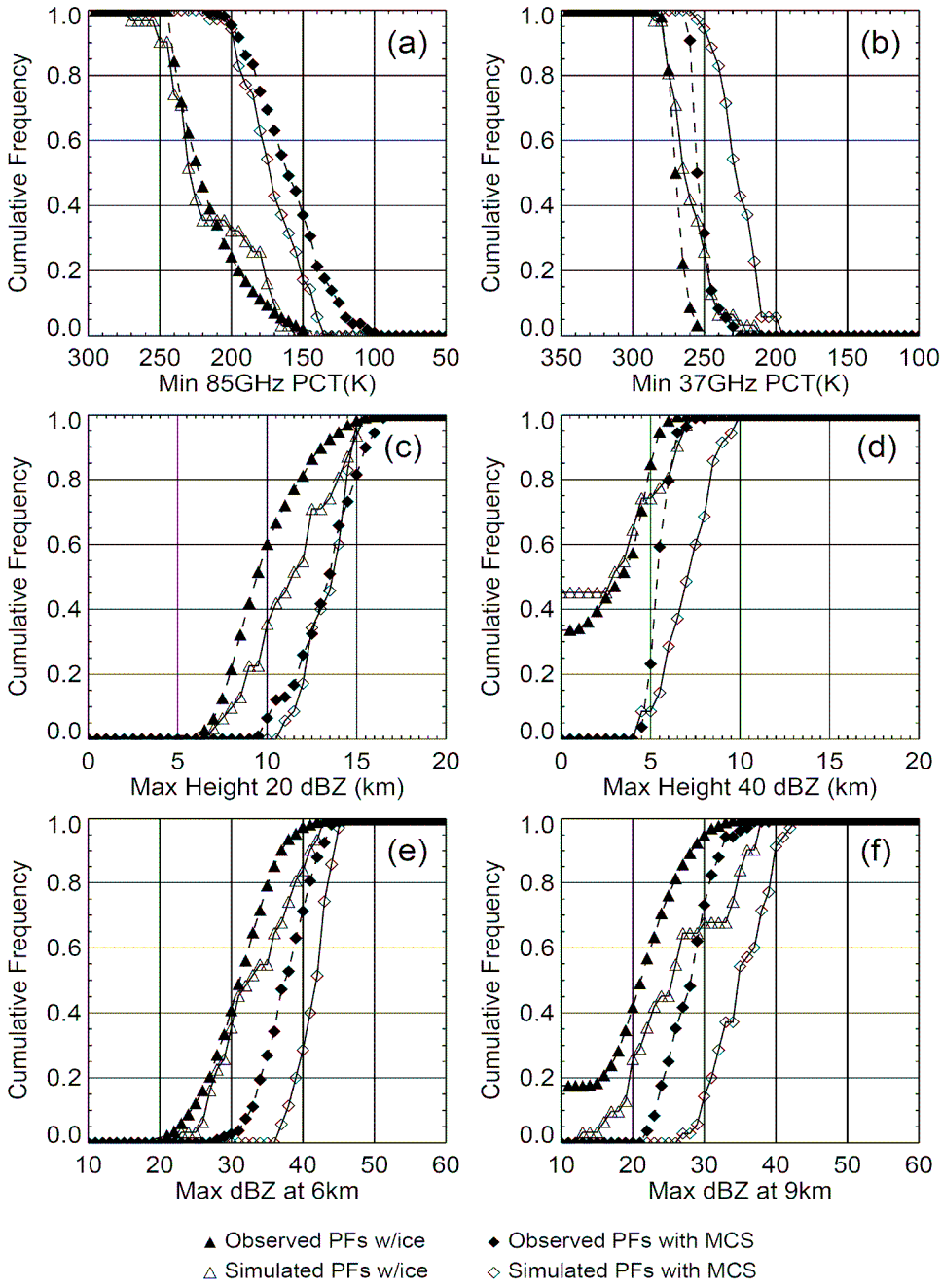

Figure 5. CDFs of (a) minimum 85-GHz PCT; (b) minimum 37-GHz PCT; (c) maximum height of the 20 dBZ echo; (d) maximum height of the 40 dBZ; (e) maximum 6-km reflectivity; (f) maximum 9-km reflectivity for TRMM observed precipitation features in the region of Kwajalein and the CRM simulated PFs during 1800 UTC August 11 to 0600 UTC August 12 1999.

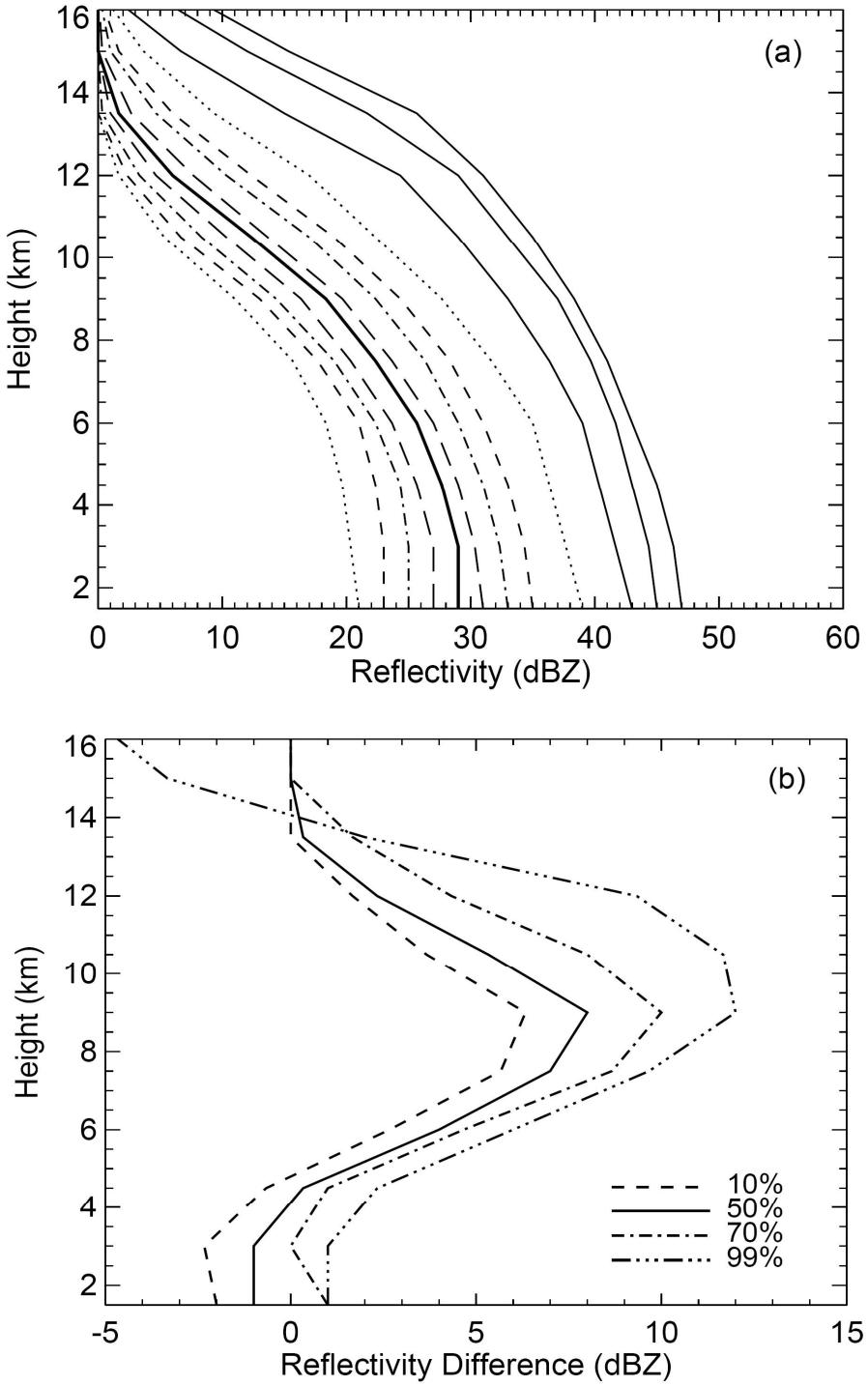

Figure 6. CCFADs for (a) the CRM simulated radar reflectivities during 2025 UTC 11 August to 0200 UTC 12 August 1999; Cumulative frequencies of a 10% quantile from 10-90%, 99%, 99.9%, and 99.99% are contoured; the 50% profile is the solid, thick line. (b) differences between the CRM simulated and the Kwajalein ground radar observed reflectivities for the KWAJEX 11-12 August 1999 precipitating system. Cumulative frequencies are shown as the legend.

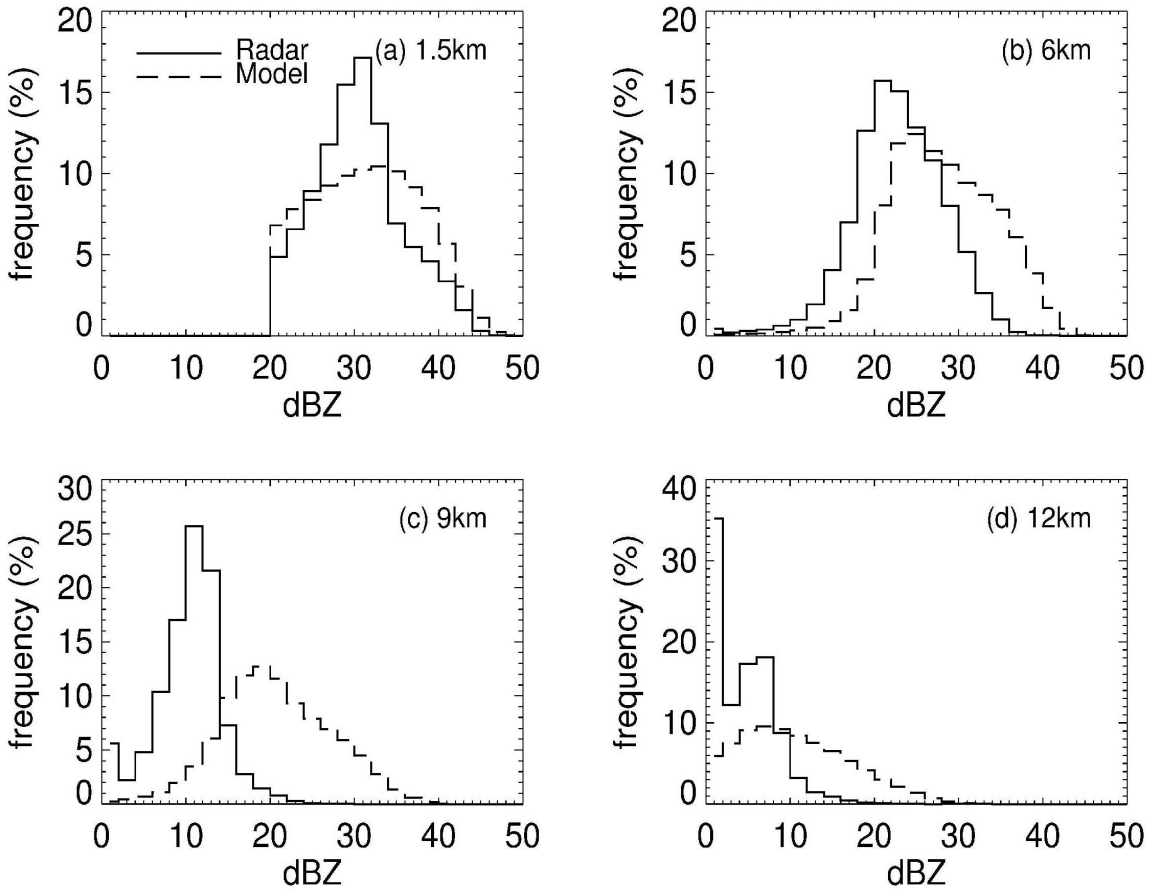

Figure 7. PDF of the Kwajalein ground S-band radar observed and the cloud resolving model simulated reflectivities (a) at 1.5 km; (b) 6 km; (c) 9 km; and (d) 12 km during 2025 UTC 11 August to 0200 UTC 12 August 1999.

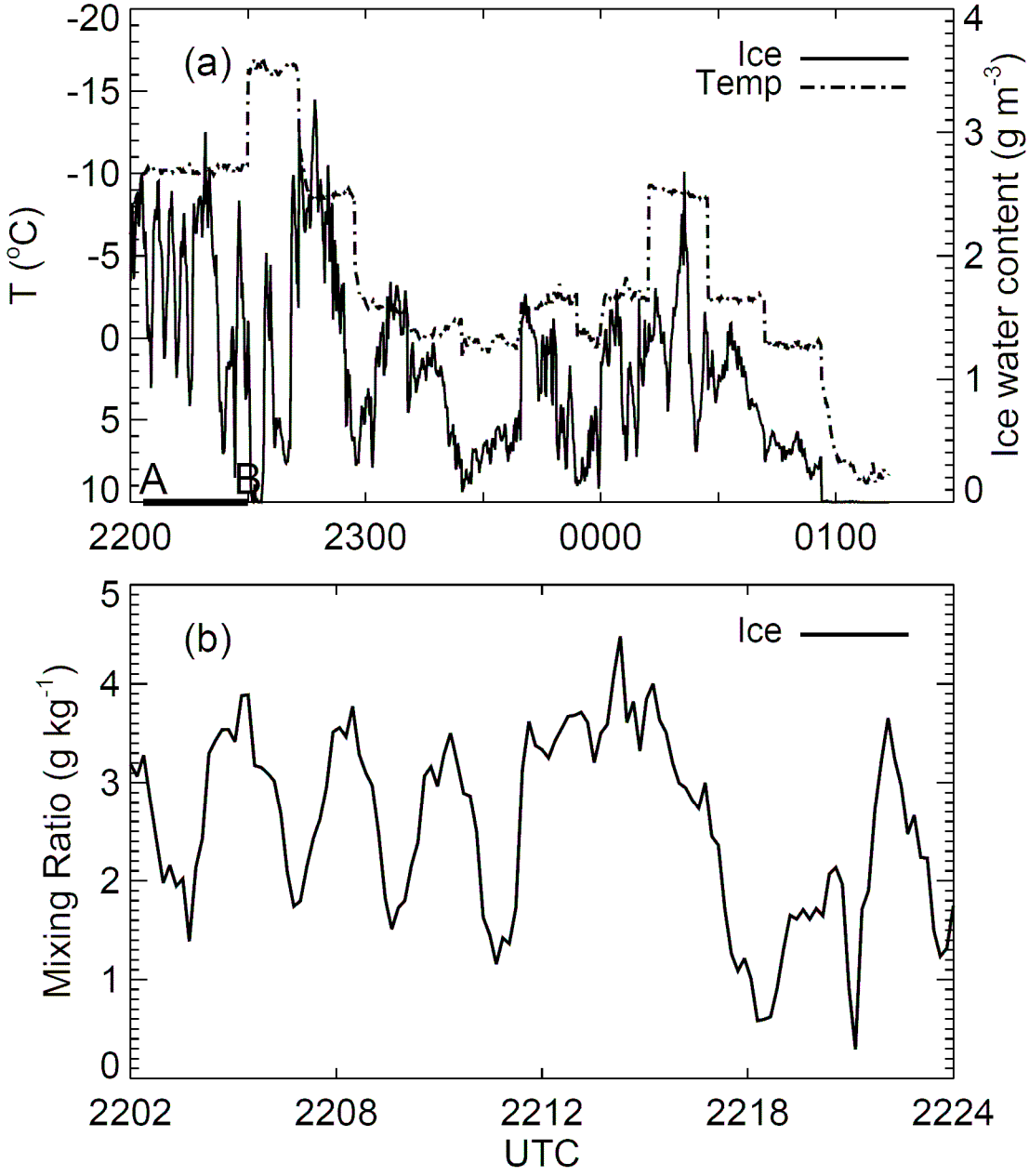

Figure 8. Time series of (a) Citation temperature and ice water content for the mission between 2200 UTC 11 August and 0131 UTC 12 August 1999 during the KWAJEX; (b) ice water mixing ratio for the 22-min period of 2202 – 2224 UTC [indicated by A-B in (a)] (at ~ 6.4 km).

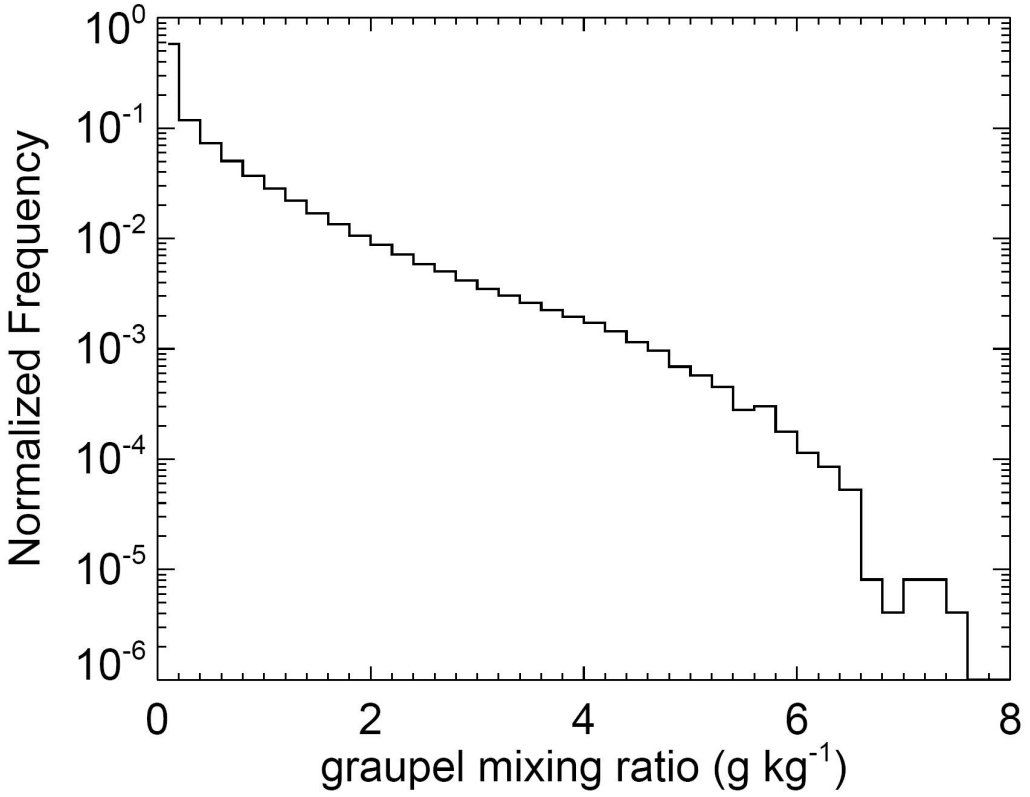

Figure 9. Histogram of frequency of occurrence of the cloud resolving model simulated graupel mixing ratio for cloudy grid points at 6.4 km during 2100 UTC to 2300 UTC 11 August 1999.